

SUPPLEMENTAL MATERIALS

for

Pt Current Collectors Artificially Boosting Praseodymium Doped Ceria Oxygen Surface Exchange Coefficients

Yuxi Ma,^{1,2} Theodore E. Burye,^{1,3} Jason D. Nicholas^{1,*}

¹ Michigan State University, Chemical Engineering and Materials Science Dept., East Lansing, MI 48824

² Contemporary Amperex Technology USA Inc, Rochester Hills, MI 48309

³ U.S. Army Combat Capabilities Development Command Ground Vehicle Systems Center, Warren, MI 48092

* Corresponding Author: jdn@msu.edu

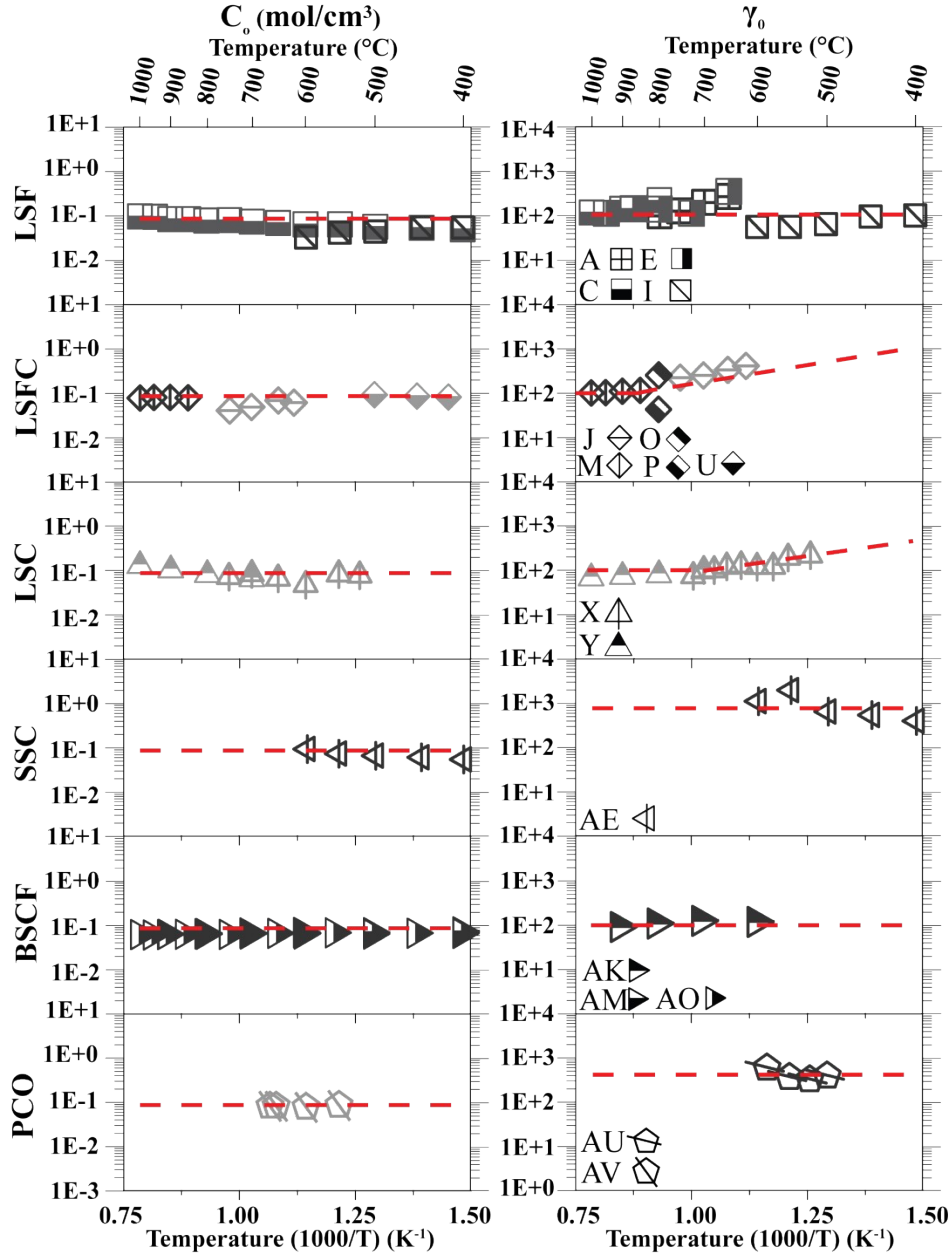


Figure S1. Lattice oxygen concentrations (left) and thermodynamic factors (right) for various oxygen exchange materials in air. Dark gray symbols represent data obtained by studies measuring both lattice constant and oxygen nonstoichiometry data or k_{chem} and k_o data. Light gray symbols represent data obtained by studies with one measured value and at least one assumed value. The red dashed lines represent the $C_o = 8.8 \times 10^{-2} \text{ mol/cm}^3$ value commonly used in the literature^{1,2} (left) or the best fit to the γ_o data (right). A = Mosleh et al.,³ C = Sogaard et al.,⁴ E = ten Elshof et al.,⁵ I = Tripkovic et al.,⁶ J = Plonczak et al.,² M = Dalslet et al.,⁷ O = Lane et al.,⁸ P = Li et al.,⁹ U = Simrick et al.,¹⁰ X = Egger et al.,¹¹ Y = Sogaard et al.,¹² AE = Yeh et al.,¹³ AK = Bucher et al.,¹⁴ AM = Girdauskaite et al.,¹⁵ AO = Wang et al.,¹⁶ AU = Ma and Nicholas,¹⁷ AV = Chen et al.¹⁸

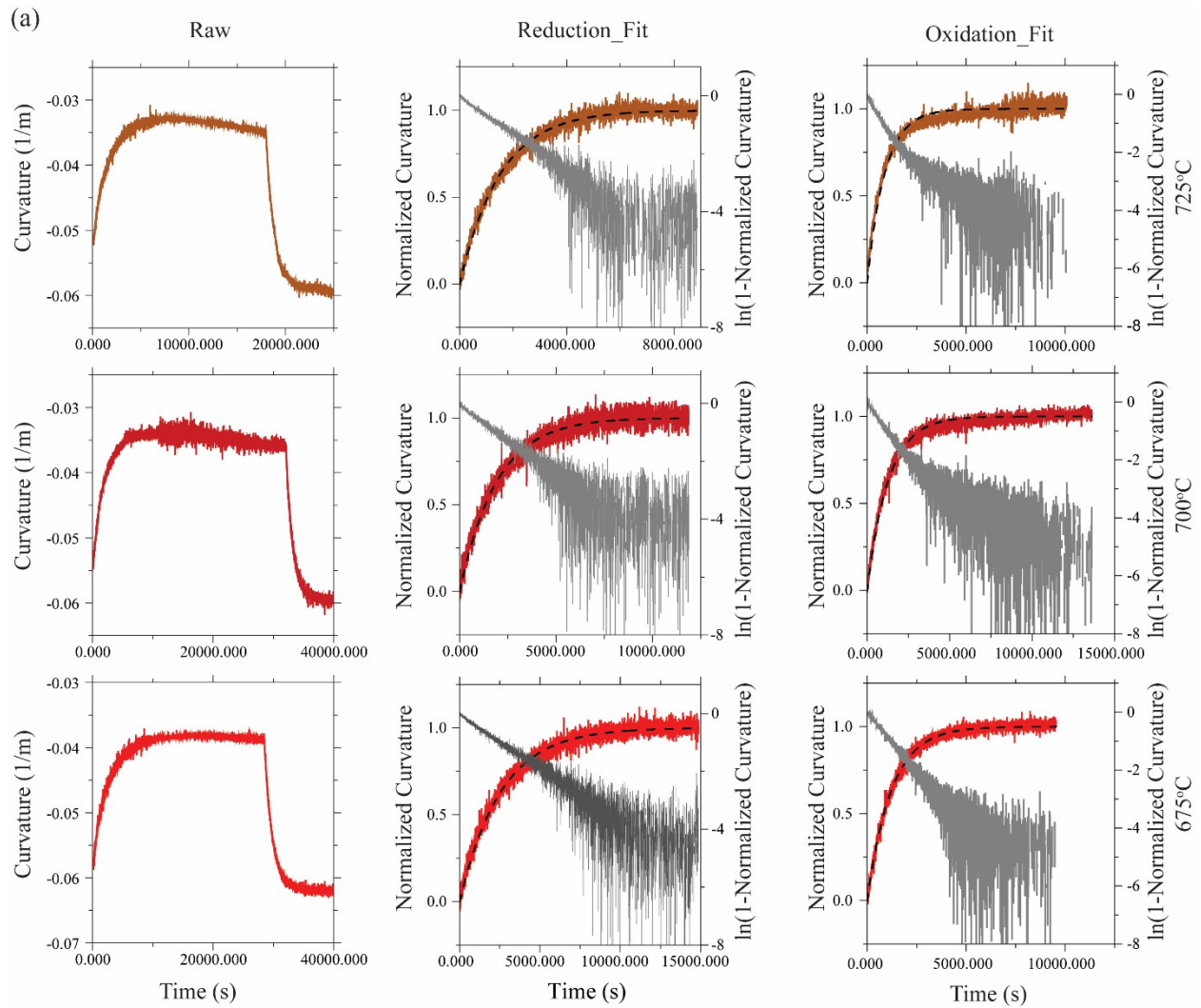


Figure S2. Representative curvature redox cycling behavior for the uncovered PCO|YSZ samples at various temperatures (left) and fits to the reduction (middle) and oxidation (right) portions of that data. Dashed curves denote curvature relaxation data replotted as a normalized curvature (i.e. the quantity found in the left portion Eqn. 3) for k_{chem} fitting via Eqn. 3. Grayed out curves denote curvature relaxation data replotted to show that only a single process, with a single time constant, was active during each relaxation.

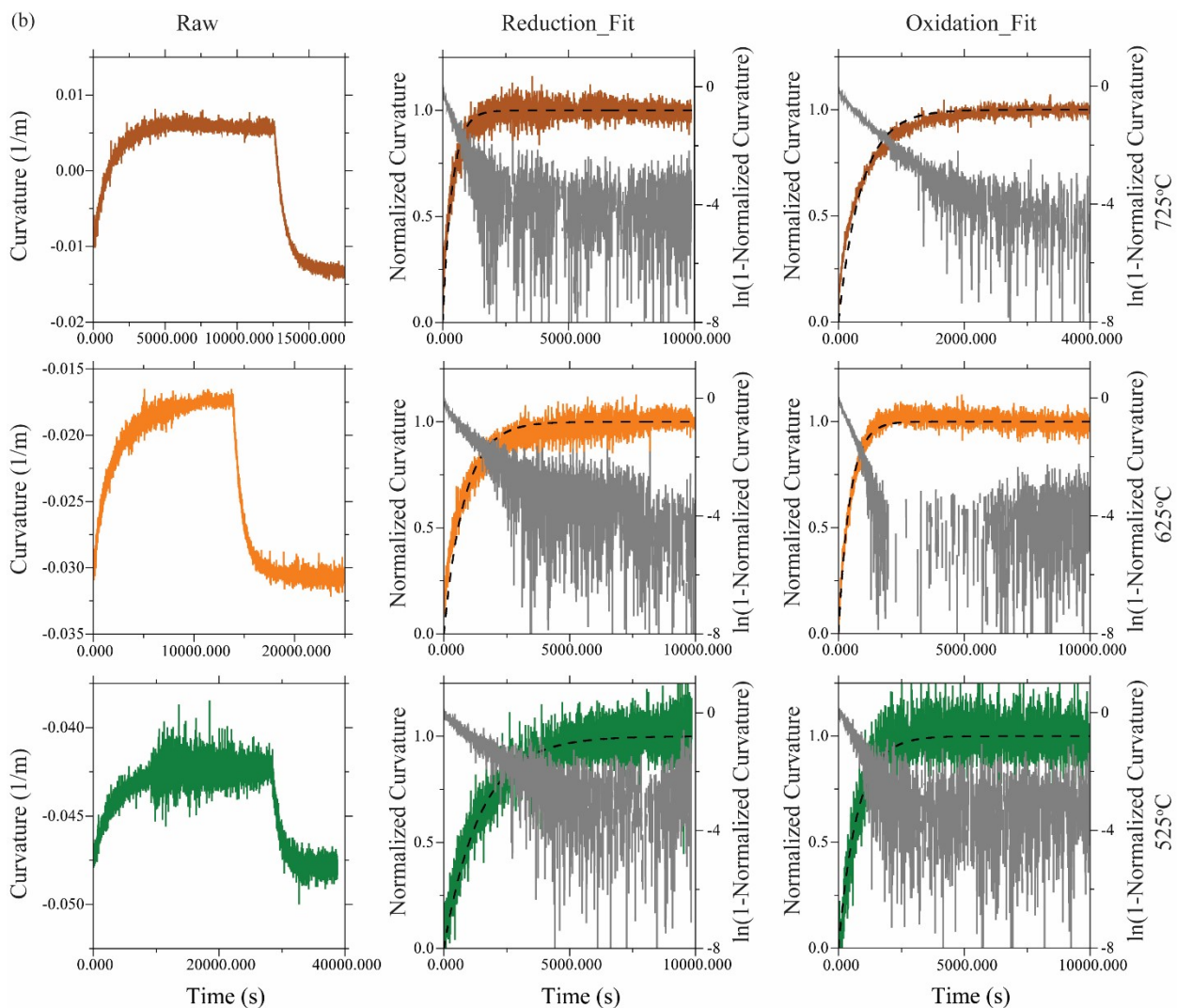


Figure S3. Representative curvature redox cycling behavior of partially-covered PCO|YSZ samples at various temperatures (left) and fits to the reduction (middle) and oxidation (right) portions of that data. Dashed curves denote curvature relaxation data replotted as a normalized curvature (i.e. the quantity found in the left portion Eqn. 3) for k_{chem} fitting via Eqn. 3. Grayed out curves denote curvature relaxation data replotted to show that only a single process, with a single time constant, was active during each relaxation.

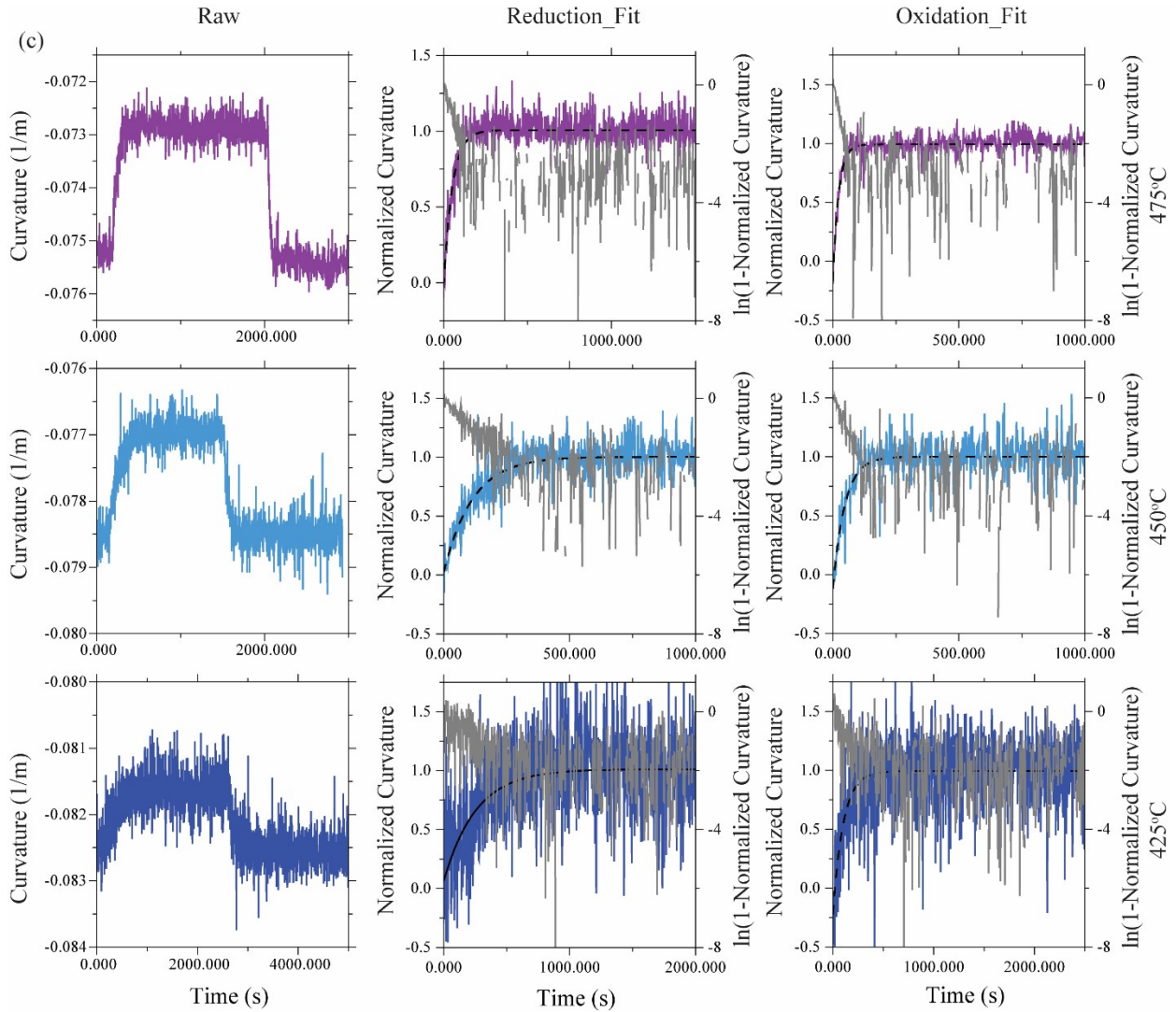


Figure S4. Representative curvature redox cycling behavior for the completely-covered PCO|YSZ samples at various temperatures (left) and fits to the reduction (middle) and oxidation (right) portions of that data. Dashed curves denote curvature relaxation data replotted as a normalized curvature (i.e. the quantity found in the left portion Eqn. 3) for k_{chem} fitting via Eqn. 3. Grayed out curves denote curvature relaxation data replotted to show that only a single process, with a single time constant, was active during each relaxation.

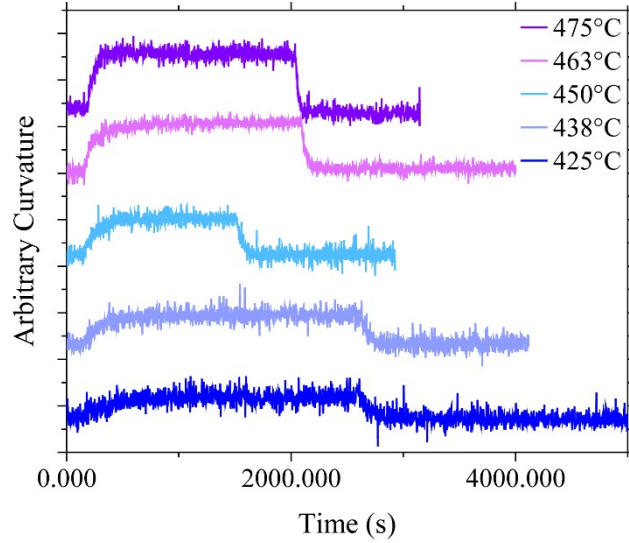


Figure S5. The curvature of the completely Pt-covered PCO|YSZ samples with oxygen partial pressure cycling from air, to 10x diluted air, and back to air. Similar data for uncoated PCO|YSZ samples can be found in Ma and Nicholas.¹⁷

Additional Equations Used to Convert Between Oxygen Surface Exchange Properties

The following equations were used, in conjunction with Eqn. 1-4, to convert between the oxygen surface exchange properties shown in Figure 1:

$$\gamma_o = \frac{(3 - \delta) * \gamma_v}{\delta}$$

[S1]

$$\gamma_o = \frac{D_{chem}}{D_o}$$

[S2]

$$C_o = \frac{\sigma_{o2} - * k_b * T}{4 * F^2 * D_o}$$

[S3]

$$C_o = \frac{3 - \delta}{V_m}$$

[S4]

$$D_o = \frac{D^*}{f} \quad [S5]$$

where C_o is the oxygen ion concentration, D_o is the oxygen ion diffusion coefficient, D_{chem} is the oxygen chemical diffusion coefficient, D^* is the oxide ion tracer diffusion coefficient, δ is the oxygen nonstoichiometry, F is the Faraday constant, f is the structural correlation factor (0.69 for the perovskite-structured materials needing conversion here), γ_o is the oxygen ion thermodynamic factor, γ_v is the oxygen vacancy thermodynamic factor, k_b is Boltzmann's constant, $\sigma_{o^{2-}}$ is the oxygen ion conductivity, T is temperature, and V_m is the molar volume. As shown in the accompanying Excel spreadsheet, whenever possible, oxygen concentration or other data needed to perform a conversion from one surface exchange property to another was taken from data collected in the same publication as the directly-measured oxygen surface exchange coefficient. As indicated in the accompanying spreadsheet, when this was not possible, data from other literature studies was used.

References

1. F. S. Baumann, J. Fleig, H.-U. Habermeier and J. Maier, *Solid State Ionics*, 2006, **177**, 1071-1081.
2. P. Plonczak, M. Søgaaard, A. Bieberle-Hütter, P. V. Hendriksen and L. J. Gauckler, *Journal of the Electrochemical Society*, 2012, **159**, B471-B482.
3. M. Mosleh, M. Sogaard and P. V. Hendriksen, *Journal of the Electrochemical Society*, 2009, **156**, B441-B457.
4. M. Søgaaard, P. Vang Hendriksen and M. Mogensen, *Journal of Solid State Chemistry*, 2007, **180**, 1489-1503.
5. J. E. tenElshof, M. H. R. Lankhorst and H. J. M. Bouwmeester, *Journal of the Electrochemical Society*, 1997, **144**, 1060-1067.
6. D. Tripkovic, R. Kungas, M. B. Mogensen and P. V. Hendriksen, *Phys. Chem. Chem. Phys.*, 2020, **22**, 15418-15426.
7. B. T. Dalslet, M. Søgaaard and P. V. Hendriksen, *Journal of the Electrochemical Society*, 2007, **154**, B1276-B1287.
8. J. A. Lane, S. J. Benson, D. Waller and J. A. Kilner, *Solid State Ionics*, 1999, **121**, 201-208.
9. Y. H. Li, K. Gerdes, T. Horita and X. B. Liu, *Journal of the Electrochemical Society*, 2013, **160**, F343-F350.
10. N. J. Simrick, A. Bieberle-Hutter, T. M. Ryll, J. A. Kilner, A. Atkinson and J. L. M. Rupp, *Solid State Ionics*, 2012, **206**, 7-16.
11. A. Egger, E. Bucher, M. Yang and W. Sitte, *Solid State Ionics*, 2012, **225**, 55-60.
12. M. Søgaaard, P. V. Hendriksen, M. Mogensen, F. W. Poulsen and E. Skou, *Solid State Ionics*, 2006, **177**, 3285-3296.
13. T. C. Yeh, J. L. Routbort and T. O. Mason, *Solid State Ionics*, 2013, **232**, 138-143.
14. E. Bucher, A. Egger, P. Ried, W. Sitte and P. Holtappels, *Solid State Ionics*, 2008, **179**, 1032-1035.
15. E. Girdauskaite, H. Ullmann, V. V. Vashook, U. Guth, G. B. Caraman, E. Bucher and W. Sitte, *Solid State Ionics*, 2008, **179**, 385-392.
16. L. Wang, R. Merkle and J. Maier, *Journal of the Electrochemical Society*, 2010, **157**, B1802-B1808.
17. Y. Ma and J. D. Nicholas, *Phys. Chem. Chem. Phys.*, 2018, **20**, 27350-27360.
18. D. Chen, S. R. Bishop and H. L. Tuller, *Journal of Electroceramics*, 2012, **28**, 62-69.